

1 Decision Support Systems for Real-World High-Speed Rail Planning

2 By Ana Laura Costa, Ph.D. ^{(1)(*)}, Maria da Conceição Cunha, Ph.D. ⁽²⁾, Paulo A. L. F. Coelho, Ph.D. ⁽³⁾, and
3 Herbert H. Einstein, Sc.D., F. ASCE⁽⁴⁾

4 ⁽¹⁾ Researcher, Department of Civil Engineering, University of Coimbra, alcosta@dec.uc.pt, ^(*) *corresponding*
5 *author*

6 ⁽²⁾ Professor, Department of Civil Engineering, University of Coimbra, mccunha@dec.uc.pt

7 ⁽³⁾ Assistant Professor, Department of Civil Engineering, University of Coimbra, pac@dec.uc.pt

8 ⁽⁴⁾ Professor, Department of Civil and Environmental Engineering, Massachusetts Institute of Technology,
9 einstein@mit.edu

11 ABSTRACT

13 The selection of the macro-location of new High-Speed Rail (HSR) systems during the planning stage affects
14 the associated infrastructure costs. The process is influenced by the complex interaction between the HSR
15 alignment, the technical solutions and the characteristics of the deployment site, subject to layout restrictions.
16 Decision-support systems for the optimization of the HSR alignment are developed for addressing the
17 requirements of large and complex real projects. The formulation includes costs, geometric constraints,
18 connection requirements and consideration of natural barriers such as protected land-use and bodies of water,
19 ubiquitous in real projects. The Simulated Annealing Algorithm is implemented to address challenges of real
20 problems and solve the optimization model. The approach is applied to a Portuguese HSR case. The solution
21 obtained optimizes its alignment by minimizing the construction costs, consistent with existing projects
22 worldwide, and complying with location, geometry and land-use restrictions. The approach is not case-specific
23 and can be used to systematically study trade-off opportunities and support decision-making in similar planning
24 problems. Alternative solutions can be generated based on different judgments on the trade-offs.

25 *Keywords:*

26 High-speed rail; Macro-location planning; Decision-support systems; Simulated Annealing Algorithm;

27 *CEDB Subject Headings:*

28 Optimization; Algorithms; High-speed rail; Alignment; Decision support systems

29

30 **Introduction**

31 When planning new High-Speed Rail (HSR) systems, initial decisions are made concerning the infrastructure
32 macro-location. Project specifics such as the type of traffic (passenger-only, freight or mixed) and the design
33 speed imply different geometric requirements (CEN 2002; EC 2008) and track displacement limits (RTRI
34 2007), which influence the HSR configuration. These project specifics coupled with site characteristics, such as
35 elevation, geology, geotechnical behavior, population density or climate, determine the technical solutions to
36 implement. Furthermore, the HSR must consider land-use in protected areas and crossing bodies of water. As
37 the site characteristics can vary significantly along a HSR line, so can the technical solutions adopted, which
38 relate to varying construction costs. Campos and de Rus (2009) compiled data from HSR projects in Europe,
39 South Korea and Taiwan observing that the construction cost per km (without planning and land expropriation
40 costs) varied between €4.7 million and €65.8 million (in 2005 euros). Moreover, the macro-location of HSR
41 systems constrains subsequent optimization processes for specific infrastructure sections and the location of
42 stations that are crucial for the HSR success (Brons et al. 2009). As a result, it is extremely difficult to obtain the
43 HSR configuration yielding the most value, particularly in the planning stage, in which large areas and
44 significantly different configurations can be considered.

45 Complex decisions need to be made, and large investments are necessary, when defining rail
46 alignments and selecting the number and locations of stations along the rail line. As discussed in the literature,
47 the optimization of the location of rail stations and the optimization of rail alignments can lead to significant
48 savings in investment costs and operation costs of rail systems while also satisfying other objectives (Kang et al.
49 2014). Extensive research exists on the optimization of rail alignments and the location of stations (Jha et al.
50 2007; Kang et al. 2014; Repolho et al. 2013; Samanta and Jha 2011). However, there are intertwined aspects of
51 HSR rail planning (Repolho et al. 2013) and a fully-integrated approach, which can also consider optional
52 intermediate stations in-between fixed terminal ones, was not found in the literature.

53 Addressing these issues, Costa et al. (2013) proposed an optimization model for HSR standard
54 planning conditions (SPC), i.e. under, ordinary operating conditions prevailing within the lifetime of the
55 infrastructure. The objective function intends to minimize construction costs and optimize geometric layout,
56 land-use and the inclusion of intermediate stations, providing a systematic approach to trade-off opportunities
57 between such factors. A user-friendly computational tool was developed to solve the proposed SPC model. The
58 tool implemented the Simulated Annealing Algorithm (SAA) (Kirkpatrick et al. 1983) for solving the model,
59 based on research by Cunha (1999) and Cunha et al. (2009). Techniques other than local search have been

60 implemented for solving the highway alignment optimization problem but limitations have been identified in
61 addressing model- and/or problem specifics (Kang et al. 2012). Within local search techniques, the SAA
62 implementation produced good results in solving similar optimization problems (Angulo et al. 2012; Marques et
63 al. 2015; Zeferino et al. 2012).

64 The optimization model by Costa et al. (2013) represented interacting factors affecting the HSR
65 planning in the conceptual stage. The conception of the model and the implementation and calibration of the
66 solving technique were illustrated for a simple and synthetic case-study. However, transitioning to real-world
67 complexity raises challenges, both for the model formulation and the implementation of the solving technique
68 (Maier et al. 2014) that this paper addresses. Larger problem size and complex interacting factors, typical of
69 real-world decision-making, develop additional difficulties that decision support systems developed for simple
70 problems do not consider. The optimization model and the solving technique need to deal with intricacies that
71 abound in real projects, and the sheer size of the problems may increase the computation burden beyond
72 tolerable bounds. While synthetic case-studies are valuable for proof of concept, the refinements of the approach
73 discussed here are required for tackling the complexities of real-world problems. This paper develops decision
74 support systems for real-world high-speed rail planning problems and its contributions address:

- 75 • Natural barriers to the infrastructure
- 76 • Effects of layout safety requirements
- 77 • Infrastructure costs

78 Based on the conceptual and operational frameworks developed, the capabilities of the approach are illustrated
79 for the specific case of the Lisbon-Oporto HSR planning problem. This HSR aims at linking Lisbon, Coimbra
80 and Porto with a passenger-dedicated double-track HSR line (Fig.1). The HSR layout configuration is
81 represented by linear sections that connect a set of sequential 3D points in space. A discretization mesh for the
82 case-study area, with a grid of 2km in plan view (x and y directions) and 10m in elevation, defines the set of all
83 permissible node positions from which a limited number is selected to be connected by the HSR line. The study
84 considers that the connection of the cities Aveiro and Leiria is optional, depending on trade-offs with additional
85 construction and operation costs. The input maps are obtained from geographic information systems.

86 **The Simulated Annealing Algorithm**

87 The Simulated Annealing Algorithm (SAA) traces its origins to the annealing process of materials to low energy
88 states and is credited to Kirkpatrick et al. (1983) who applied the Metropolis concepts (Metropolis et al. 1953) to
89 solve the travelling salesman problem. Costa et al. (2013) overview the algorithm and comprehensive

90 discussions are presented in the literature (Aarts et al. 1997; Van Laarhoven and Aarts 1987). Concisely, the
91 algorithm starts with an initial system configuration, and neighboring configurations are tested and accepted as
92 current configurations if they improve the value of the objective function. Worsening system configurations are
93 also accepted as current configurations with a probability based on the Metropolis criteria, allowing the SAA to
94 escape from local optima. The SAA is as a stochastic technique that applies a probabilistic mechanism for
95 accepting worse solutions (Aarts et al. 1997). However, even if the algorithm is disassociated from the physical
96 meaning, the terminology borrowed from the annealing physical process is used (Johnson et al. 1989). The
97 probability of accepting worsening configurations decreases as the algorithm progresses (cooling) at descending
98 values of a control parameter (temperature).

99 **Implementation of the Simulated Annealing Algorithm**

100 Based on the SAA principles, three main elements are necessary for an implementation of the algorithm: a set of
101 parameters governing the convergence of the algorithm (cooling schedule), an initial system configuration, and
102 the procedures to generate new candidate configurations within a neighborhood structure. The initial system
103 configuration and the generation of new candidate configurations are problem-specific. For the Lisbon-Oporto
104 case, the HSR solutions are defined by a linear alignment connecting a set of sequential nodes. Feasibility
105 requires that nodes representing the cities of Oporto, Coimbra and Lisbon are connected (Fig.1), and that
106 applicable regulatory and safety requirements for geometric design and land-use restrictions are complied with.

107 **Cooling Schedule**

108 The cooling schedule of the SAA defines the finite sequence of values of the temperature (control parameter)
109 and a finite number of transitions at each temperature by specifying (Aarts et al. 1997):

- 110 • an initial value of the temperature t_0 ;
- 111 • a decrement function for lowering the temperature;
- 112 • the finite length of each homogeneous Markov chain, meaning a minimum number of iterations n_l to be
113 performed at each temperature step;
- 114 • a termination criterion for the algorithm.

115 While the SAA may be applied to solve a wide range of problems, the algorithm parameters producing the best
116 solutions in each case depend on the problem solved and its size (Johnson et al. 1989). Pardalos et al. (2000)
117 discuss the difficulty of choosing a cooling schedule, as its performance for a particular problem cannot be fully
118 appreciated *a priori*. The choice relies on an adaptive geometric (Johnson et al. 1989), as implemented by Costa
119 et al. (2013) based on research by Cunha (1999), Cunha et al. (2009) and Johnson et al. (1989). Each k^{th}
120 temperature decrease step is governed by $t_k = r^k \times t_0$, with a decrease rate r and an initial temperature $t_0 = -0.1$

121 $c(s_0)/\ln(a)$, where $c(s_0)$ is the value of the objective function of the initial configuration and a is the elasticity of
122 acceptance defining the probability of accepting a worsening solution at the initial temperature step. The SAA is
123 terminated if n_2 consecutive temperature decrease steps do not improve either the optimum or the average value
124 of the HSR configurations.

125 **Initial System Configuration**

126 Different possible methodologies can be used for defining an initial system configuration such as the use of
127 heuristics (Johnson and McGeoch 1997) or an arbitrarily random or best guess configuration (Bertsimas and
128 Nohadani 2010). However, if the SAA implementation allows one to conduct the global search of the feasible
129 space, the initial configuration will not interfere with the accessibility of the search space nor interfere with the
130 quality of the final solution (Bertsimas and Nohadani 2010). Given the significant overhead computation time
131 associated with random- and heuristic- generated configurations, the case-study implements an arbitrary user-
132 specified, feasible initial HSR. Feasibility ensures compliance with the problem constraints; at this stage, they
133 are mandatory connections, land-use and geometry of the alignment, but further model developments can
134 impose additional requirements.

135 **Generation of New System Configurations**

136 Consider the definition of the discretization mesh Ω_N (Fig. 2) whose vertices represent the permissible 3D
137 positions for the nodes defining the HSR alignment. Obtaining a new candidate HSR alignment consists of
138 defining a new set of nodes and their respective linear sections. The neighborhood structure thus defines the
139 maximum envelope distance at which each node can be repositioned.

140 Fig. 2a illustrates the 3D neighborhood of a current (center) node of Ω_N within its discretization mesh.
141 Moves are allowed to any of the adjacent nodes varying x, y and/or z that define the neighborhood envelope.
142 Nodes that are mandatorily connected by the HSR (see location constraint by Costa et al. (2013)) have particular
143 neighborhood structures. In the case-study, Oporto, Coimbra and Lisbon are the mandatory nodes with a fixed
144 location and moves of any kind are disallowed.

145 The plan view of Fig. 2b shows a current configuration (formed by linear sections c1, c2 and c3)
146 connecting the mandatory start and end nodes that is perturbed into a neighboring configuration (formed by
147 linear sections n1, n2 and n3). The plan view of sections c3 and n3 coincides. Note that even if three-
148 dimensionally coincident, the construction costs of sections c3 and n3 are not necessarily equal. The technical
149 solutions adopted for the cross-section govern the construction cost and these can vary for two linear sections
150 with identical 3D alignment. For example, if a bridge is required in the new section n2, it may be extended into
151 a part of section n3, while sections c2 and c3 require only embankments. This emphasizes the continuity

152 required in the cross-sections, for which the technical solution at a given point may be influenced by those
153 required upstream and downstream of that point.

154 The generation of new candidate HSR configurations aims at allowing small rearrangements to be
155 tested instead of profound changes. This is affected by the neighborhood structure but also by the degree of
156 freedom with which the current configuration is perturbed. In the case of the HSR optimization problem, the
157 degree of freedom relates to the number of nodes to be randomly perturbed to generate a new alignment. If the
158 degree of freedom is too low, the algorithm can be circumscribed to part of the design space, but if the degree of
159 freedom is too large, the algorithm engages in a random search and refrains from taking advantage of the local
160 neighborhood search properties (Jilla and Miller 2001). Based on preliminary studies for the Portuguese case,
161 the SAA implementation perturbs two random nodes of the current HSR configuration.

162 **Addressing Real-World Complexity**

163 Additional challenges develop when aiming at solving real-world HSR planning problems. The model
164 formulation can only realistically represent the problem if existing conditions such as crossing bodies of water
165 and determinant construction costs are accounted for. On the other hand, the solving technique is required to
166 address such model complexities and large datasets. The SAA is implemented based on the framework
167 discussed in the previous section but real and complex problems require that a specific implementation be
168 tailored. These issues are now discussed and illustrated for the specific case of the Lisbon-Oporto HSR line
169 based on real data (RAVE 2008).

170 ***Natural Barriers***

171 **Land-Use**

172 Different land-use areas, irregularly sized and shaped, exist in real problems. Specific areas can be protected
173 under regulatory frameworks and HSR overlay may be barred. When such areas are scattered within the search
174 space of the problem, the ability of the SAA to perform a global search can be limited and, as a result, the ability
175 of the algorithm of finding optimal or near-optimal solutions is compromised.

176 Land-use challenges to the algorithm convergence are identified for the Lisbon-Oporto case (Fig. 3)
177 where protected land-use exist, in which HSR overlay is not allowed. Starting from an initial arbitrary HSR
178 (Fig. 3a), under the current procedures for generating new system configurations, an implementation of the SAA
179 results in a sub-optimal solution (Fig. 3b), as later proven. The algorithm is able to search the problem space in
180 multiple positions relative to the smaller protected areas but larger protected areas act as barriers that the SAA
181 implementation cannot overcome. This limits the SAA ability to perform a global search within the feasible

182 space of the problem, hindering the algorithm convergence to global optima.

183 Advanced mechanisms are adopted for the generation of new candidate configurations that eliminate
184 the restrictions posed to the SAA convergence by the protected land-use. One major difficulty of the process is
185 to account for the constraints that limit the minimum horizontal angles (proxy for radii) at intermediate nodes of
186 the HSR configurations when generating new HSR alignments. These constraints aim at ensuring a smooth
187 change of direction in plan view, as required for the high operating speeds. Consider the example of Fig. 4, for
188 which the current node N is randomly chosen to be horizontally repositioned to the right (N') by the spacing of
189 the discretization mesh δ . If a small area of protected land-use exists (Fig. 4a), the move to N' can successfully
190 avoid the protected area. However, for a larger area (Fig. 4b), this repositioning distance ($\Delta_1=\delta$) is not sufficient,
191 as the candidate configuration still overlays the protected area.

192 The procedures adopted consist in incrementing the repositioning distance of node N in the original
193 direction. Fig. 4b shows that repositioning does not avoid the area unless $\Delta_3=\delta$. However, this shift leads to
194 increasingly smaller, not acceptable horizontal angles at nodes N' , N-1 and N+1. Hence, a new candidate
195 configuration obtained with the incremental displacement may be infeasible if not complying either with the
196 land-use constraint or the horizontal angle constraint. In this latter case, a new tentative generation procedure is
197 considered, which also repositions the anterior and posterior nodes. Fig. 4c shows how the alignment from Fig.
198 4b can be successfully transposed by repositioning the nodes N, (N-1) and (N+1).

199 Given that the algorithm implementation may have to consider various shapes and sizes of protected
200 areas, a general procedure is developed. It consists of the tentative generation of feasible HSR configurations in
201 five sequential steps and stops when a feasible configuration is reached. It aims at defining a new candidate
202 configuration that smoothly repositions itself in relation to the protected land-use area but can still be framed
203 within the neighborhood principles of the SAA. The steps involve the repositioning of a number of anterior and
204 posterior nodes in addition to the randomly chosen node N. In each step, the displacement of N is incremented
205 until a feasible configuration is found. If the displacement causes non-compliance with the horizontal angle
206 constraint, or the repositioning distance extends beyond the search space of the problem, the current step stops
207 and the subsequent step starts. The detailed sequence of these steps is presented below.

- 208 • Step 0: only node N is displaced and sequentially incremented (Fig. 4a).
- 209 • Step 1: nodes N, (N-1) and (N+1) are displaced (Fig. 4c). (N-1) and (N+1) are repositioned at 1/2 of the N
210 displacement, in the same direction.
- 211 • Step 2: nodes N, (N-1), (N-2), (N+1) and (N+2) are displaced (Fig. 5a). (N-1) and (N+1) are repositioned

212 at $2/3$ of the N displacement and $(N-2)$ and $(N+2)$ are repositioned at $1/3$, all in the same direction as N . It
213 should be noted that the problem discretization requires all node positions to correspond to a node in Ω_N .
214 Thus all repositioning distances are rounded to the closest multiple of δ , as exemplified in Fig. 5a.

- 215 • Step 3: nodes N , $(N-1)$, $(N-2)$, $(N-3)$, $(N+1)$, $(N+2)$ and $(N+3)$ are displaced (Fig. 5b). $(N-1)$ and $(N+1)$ are
216 repositioned at $3/4$ of the N displacement, $(N-2)$ and $(N+2)$ are repositioned at $1/2$ of the N displacement
217 and $(N-3)$ and $(N+3)$ are repositioned at $1/4$ of the N displacement, all in the same direction as N .
- 218 • Step 4: nodes N , $(N-1)$, $(N-2)$, $(N-3)$, $(N-4)$, $(N+1)$, $(N+2)$, $(N+3)$ and $(N+4)$ are displaced. $(N-1)$ and
219 $(N+1)$ are repositioned at $8/9$ of the N displacement, $(N-2)$ and $(N+2)$ are repositioned at $7/9$ of the N
220 displacement, $(N-3)$ and $(N+3)$ are repositioned at $2/9$ of the N displacement and $(N-4)$ and $(N+4)$ are
221 repositioned at $1/9$ of the N displacement, all in the same direction as N . The displacement of N is
222 incremented until a feasible configuration is found, but if it causes the non-compliance with the horizontal
223 angle constraint or the repositioning extends beyond the search space of the problem, Step 4 is abandoned.
224 At this point, the generation of HSR candidate configurations is restarted and a new node N is randomly
225 chosen to be displaced in its neighborhood (Figure 2).

226 **Bodies of Water**

227 Bodies of water such as rivers or lakes commonly affect transport infrastructure projects. In fact, establishing
228 HSR links often involves building bridges and tunnels to overcome such natural barriers. In specific cases, the
229 bodies of water can be part of waterway routes, and navigability concerns are imposed on the construction of
230 new infrastructure. Such is the case of the Lisbon-Oporto HSR that inevitably entails the construction of bridges
231 or tunnels (Fig. 6). Furthermore, navigability is required in parts of the Tagus River.

232 To realistically represent such concerns, additional constraints are implemented in the optimization
233 model that require bodies of water to be crossed by either bridges or tunnels. These feasibility requirements
234 further determine a minimum clearance to be observed that should be defined depending on the problem
235 specifics and on hydrological studies. The Lisbon-Oporto case study defines a minimum clearance of 5m for
236 bridges crossing water, but additional navigability clearances are considered for the Tagus River. Considering
237 the characteristics of existing bridges crossing the Tagus River, a minimum height of 70 meters should be
238 complied with for additional planned bridges (Fig. 6). This makes it possible for the SAA to perform a global
239 search of the feasible space based on realistic solutions.

240 **Effects of Layout Safety Requirements**

241 Radii of horizontal curves of the HSR layout should be planned as large as feasible and should follow regulatory

242 minimum values (CEN 2002). Large centrifugal acceleration of trains, increasing with increasing speed and
243 decreasing radii, intensifies the degradation of the track, passenger discomfort and, in extreme cases, favors
244 conditions leading to train derailment (Profillidis 2006). The problem formulation considers a minimum
245 horizontal angle at any intermediate angle of the HSR alignment as a proxy for the radii (see Costa et al. 2013).

246 Preliminary applications to the Lisbon-Oporto problem, however, identify problematic effects of safety
247 requirements propagating into the optimized solution found by the SAA. These effects are herein presented,
248 followed by the procedures implemented to avoid them. Fig. 7 shows the formation of a cluster near Oporto, a
249 group of three or more closely positioned nodes connected by the HSR, causing small angles between linear
250 sections without advantage to the HSR configuration. This would hardly produce an optimal or near-optimal
251 solution of a real-world HSR: the operating speed is severely limited when changing direction and that would
252 imply slow movement through clusters, which is in contrast to the fundamental principles of HSR. These are
253 geometric considerations of the problem that interfere with the SAA implementation. Node clusters have
254 underlying effects on the HSR configurations generated and tested by the algorithm that, in turn, influence the
255 quality of the solutions produced.

256 However, when solving the optimization model, it is difficult to prevent node clusters, with speed
257 restrictions and present in the current configurations, from propagating to the generated candidate
258 configurations. Closely positioned nodes become interlocked and moves in the neighborhood are confined by
259 the horizontal angle feasibility. Furthermore, at the low temperature stages of the SAA, in which the probability
260 of accepting worsening configurations is also low, the HSR configurations required for such an elimination may
261 be rejected by producing excessively large objective function values. In fact, if a cluster forms and propagates to
262 low temperature stages of the SAA implementation most of the moves that would reverse the cluster are either
263 forbidden due to the horizontal angle feasibility requirements or will not be accepted because the probability of
264 accepting worse solutions is very low. It is possible but difficult to eliminate the clusters of speed restrictions.

265 To prevent such problematic effects and their propagation into the optimized HSR configurations, a
266 minimum length for the HSR linear sections is defined. This minimum length is intended to disallow candidate
267 configurations in which the nodes are closely positioned, thus avoiding the cluster formation, but should not be
268 so large as to compromise the SAA ability to perform a global search of the problem space.

269 A separate study was performed for the Lisbon-Oporto problem to identify the minimum length of the
270 linear sections that allow the use of circular curves with 4500 m radius (Fig. 8): the arc is required to be tangent
271 at each end to the respective linear sections while having a limited external secant Δ . The latter ensures that the

272 simplified HSR representation by linear alignments optimized by the model is in fact spatially related to the real
273 HSR defined by curves and linear sections. This simplified representation of the model can capture the main
274 features concerning the plan view and longitudinal profile for the macro-location planning, however, subsequent
275 detailed studies are needed to define the circular and transition curves forming the HSR line. Based on the
276 separate study, a minimum length of 4000 m is considered for the linear sections forming the Lisbon-Oporto
277 HSR alignment.

278 **Infrastructure Costs**

279 HSR components, such as track, ballast or catenary exist, for which the unit construction costs do not vary
280 significantly with the *in situ* characteristics. While these length-dependent costs do not add major complexities
281 to the model, their incorporation favors shorter configurations, which real projects aim at. The optimization
282 model developed for real problems includes these length-dependent costs that not only affect construction cost
283 but also relate to operating considerations. The length-dependent costs, together with the costs of crossing
284 bodies of water acting as natural barriers, with bridges or tunnels, are decisive considerations for an adequate
285 representation of the construction costs of HSR systems.

286 **Solving Real Problems: The Case of the Lisbon-Oporto HSR**

287 Spatial data are input in the form of digital raster maps for the 147.4×304.4 km² study area (Fig. 1). The raster
288 maps for protected areas, lithology and ground use (APA 2012), for bodies of water (SNIRH 2012) and for
289 elevation are discretized in 200m square geo-referenced cells. The discretization mesh, defining the feasible
290 node positions of the HSR, is formed by a grid of 2km in the plan view and 10m in elevation (Fig. 2a), between
291 elevations -50m and 1420m. The optimization model applied to the Lisbon-Oporto HSR case-study aims at the
292 minimization of the value of the objective function represented in a simplified form by eq. 1.

$$293 \quad \text{Objective Function Value} = C_{\text{Construction}} + P_{\text{HorizAngle}} + P_{\text{Gradient}} - V_{\text{InterCities}} \quad (1)$$

294 Where $C_{\text{Construction}}$ is the construction cost including expropriation, earthworks (cuts and embankments), bridges,
295 tunnels and length-dependent costs, $P_{\text{HorizAngle}}$ is a penalty for adopting horizontal angles smaller than best
296 practice design value, P_{Gradient} is a penalty for adopting longitudinal gradients larger than best practice design
297 value and $V_{\text{InterCities}}$ represents the added value of connecting intermediate and optional cities.

298 Safety requirements impose mandatory limits on geometry that are less restrictive than best practice
299 geometry design, but have implications on operation. This results in the definition of two values for each
300 geometry parameter (CEN 2002): maximum (or minimum) limit values, which are extreme but permissible
301 values that should be used in design as infrequently as possible, and recommended values consisting of best

302 practice geometry design. The absolute safety limits defining the feasibility of the HSR, in our case are a
303 minimum horizontal angle of 120° at any intermediate node of the HSR and a maximum gradient of 35 mm/m
304 for the linear sections in the longitudinal profile. The penalties in the objective function (Costa et al. 2013) are
305 related to adopting geometry parameters that are less desirable than best practice. The recommended design
306 parameters considered in the case-study are 140° and 20 mm/m. The optional connection of Aveiro and Leiria is
307 also considered through a term in the objective function. The value of connecting each city represents effects
308 such as the ability to influence ridership through increased accessibility but also possible negative effects of
309 intermediate stops causing an increase in connecting times (Repolho et al. 2013), as well as critical political
310 decisions (Levinson 2012) regarding the location of HSR stations. In addition to the geometry constraints,
311 feasibility is determined by protected areas (Fig. 3), the mandatory connection of Lisbon, Coimbra and Oporto
312 and the bridge and tunnel requirements for crossing bodies of water.

313 The SAA is implemented to solve the model and address the complexities posed by real problems. An
314 extensive study is performed to establish the cooling schedule parameters discussed earlier in the SAA
315 implementation section, analogously to the study performed by Costa et al. (2013) that compares the
316 performance of the algorithm for different values of each parameter. The cooling schedule parameter set ($a=0.9$;
317 $r=0.8$; $n_1=5000$; $n_2=10$) is observed to be the most effective for the Lisbon-Oporto case study. The plan view of
318 the initial configuration is shown in Fig. 3a. The best solution found by the algorithm is shown in the plan views
319 of Fig. 9: a) the land-use map, b) the main rivers map and c) the elevation map. The HSR connects Oporto,
320 Aveiro, Coimbra, Leiria and Lisbon. Note that the connection of Aveiro and Leiria is not mandatory but
321 depends on the user-specified benefit attributed to the connection of each of these cities. The present study
322 includes these in a cursory manner based on Costa et al. (2013), to illustrate the capabilities of the model.
323 Detailed studies can be performed for a comprehensive representation of the value of intermediate connections.

324 Fig. 9a shows that the proposed methodology for generating HSR candidate solutions is capable of
325 addressing the difficulties caused by protected land-use areas acting as natural barriers, which is not possible
326 with previous implementations (Fig. 3b). The mechanisms implemented allow the SAA to perform a global
327 exploration of the problem space, considering radically different configurations, which is central to the
328 effectiveness of finding optimal or near-optimal solutions of optimization problems. As a result, the objective
329 function value was reduced from 2008.2 (Fig. 3b) to 786.96 Million Euros (Fig. 9a).

330 Fig. 9a also compares the plan view of the HSR solution with the existing conventional railway
331 connecting Lisbon and Oporto. The lower operating speed considered for the design of the older conventional

332 railway is compatible with smaller radii of horizontal curves that, along with detours for connecting smaller
333 towns in-between major centers, results in the sinuous plan-view shown in Fig. 9a. Apart from the horizontal
334 curvature and the connection of smaller towns, both the HSR and the conventional rail share a common corridor
335 between Oporto and just south of Coimbra and also near Lisbon. One observes that by running adjacent to the
336 Atlantic Ocean, between Oporto and Aveiro, close to the Mondego River, south of Coimbra, and along the
337 Tagus River, next to Lisbon (Fig. 9b), both rail infrastructures take advantage of the smaller costs of building on
338 level ground (Fig. 9c). Fig. 10 shows the HSR longitudinal profile and ground elevation along the alignment,
339 with identification of tunnels and bridges. Note, however, that building embankments and cuts over alluvium, in
340 the flatter areas constituting the floodplains of the Mondego and Tagus Rivers, would produce some important
341 geotechnical concerns with implications on both the construction and operation phases. These should be further
342 studied in detail.

343 The HSR is 296.3km long, and tunnels are mostly built between km270 and km285 where high
344 elevations with sharp variations impose the need for tunnels (Fig. 10). Bridges are built along the alignment due
345 to both topography and crossing bodies of water, ensuring a minimum of 5m clearance for the latter. The HSR
346 does not cross the Tagus River and thus its navigability is not affected. While bodies of water may be crossed by
347 either bridges or tunnels, bridges are usually less expensive and are favored by the optimized solution when
348 technically viable.

349 The plan views of Fig. 9 also show that two pronounced curves exist in the HSR alignment around
350 Coimbra. This increases the HSR length by deviating from a more direct straight path south of Coimbra and
351 increases the length-dependent construction costs. This sinuosity, however is associated with trade-offs between
352 several cost factors constituting the objective function, namely, the curvature penalty (see expression (1)), on the
353 one hand but avoiding, on the other hand, major construction in urban areas (Fig. 11), with larger expropriation
354 costs. It also reduces the construction costs of bridges and tunnels by running on the flatter ground parallel to the
355 Mondego River (Fig. 9b and c).

356 The resulting construction costs in 2008 Euros are shown in Fig. 12. It should be noted that the
357 construction costs differ from the objective function value (eq. 1), the latter also representing geometry
358 considerations and the value of intermediate connections. The aggregate total construction cost of the HSR is
359 €1,658.50 million. Earthworks are the largest partial construction cost representing 27% of the total, followed by
360 bridges (26%), length-dependent costs (21%), tunnels (17%) and the cost of land expropriation (9%). The fact

361 that length-dependent costs are larger than those of tunnels and expropriation shows how length-dependent costs
362 can exert a significant influence on the analysis.

363 An analysis is performed to investigate how the derived costs compare with costs of existing HSR
364 projects. Campos and de Rus (2009) discuss upper and lower bounds of average construction costs per kilometer
365 (in 2005 Euros) of new and operating HSR lines around the world. The cost bounds vary significantly with *in*
366 *situ* conditions and project specifics, even when singular projects of considerable complexity are excluded: in
367 Italy costs vary between 14 and 65.8 million Euros (lines under construction), in France between 4.7 and 18.8
368 million Euros (lines in service) and in Spain between 7.8 and 20 million Euros (lines in service). An analogous
369 comparative cost for the case-study solution can be estimated at 5.61 million per km (in 2005 Euros), which is
370 close to cost average values of existing HSR projects (Campos and de Rus 2009). While the aim of the decision-
371 support systems is to derive optimal HSR configurations based on interrelated factors additional to the
372 construction costs, budget limitations exist. In this framework, the construction costs from the Lisbon-Oporto
373 HSR are consistent with the costs observed in real-world projects.

374 **Conclusions**

375 Planning for High Speed Rail (HSR) infrastructure macro-location requires that a complex interrelation of
376 spatially variable factors are accounted for. These include regulatory frameworks for infrastructure and land-use,
377 the economic and social value of the intermediate connections and the investments required for building and
378 operating HSR infrastructure. An integrated consideration of such elements is paramount in planning for
379 infrastructure. Previous conceptual studies proposed an optimization model for such an approach and sound
380 results were obtained for a simple and synthetic case-study. However, solving real problems emphasizes the
381 need for addressing additional complexities, but also introduces additional concerns to be modeled.

382 This paper proposes a decision-support system for real-world problems. The definition of the HSR
383 configuration and the connection of intermediate locations are intertwined aspects of the problem that the model
384 can address for macro-location decisions. The challenges posed by natural barriers including protected land-use
385 and crossing bodies of water are addressed. Mechanisms are implemented that enable one to conduct a
386 comprehensive search of the problem solutions irrespective of existing land-use barriers. Crossing bodies of
387 water is established with the construction of bridges and tunnels and navigability concerns are introduced where
388 necessary. Moreover, the optimization model formulation includes length-dependent costs and the costs of
389 crossing bodies of water that influence the infrastructure alignment and are essential for representing real HSR
390 projects.

391 The capabilities of the approach are illustrated for the Lisbon-Oporto HSR planning. The results
392 obtained show the approach's ability to represent the characteristics of real problems and obtain valuable
393 solutions. Overall it is shown how the HSR solution optimizes its alignment by minimizing construction costs,
394 which are consistent with existing HSR projects worldwide, while addressing land-use, geometry and location
395 issues. The approach can be used to systematically study trade-off opportunities and support decision-making.
396 Alternative solutions can be generated based on different judgments on the trade-offs. The approach is not case-
397 specific and can be applied to other HSR and similar transportation planning problems. Further developments
398 may consider additional technical solutions and should incorporate operating conditions.

399 **Acknowledgements**

400 The research was carried out at the University of Coimbra and the Massachusetts Institute of Technology with
401 the financial support of the Government of Portugal through the MIT|Portugal Program and FCT doctoral grant
402 (Grant No. SFRH/BD/43012/2008), co-financed by the European Social Fund (ESF) through POPH – Programa
403 Operacional Potencial Humano. The authors also acknowledge the access to preliminary studies provided by
404 former RAVE – Rede Ferroviária de Alta Velocidade, S.A.

405 **References**

- 406 Aarts, E., Korst, J., and Van Laarhoven, P. J. M. (1997). "Simulated Annealing." *Local Search in Combinatorial*
407 *Optimization*, John Wiley & Sons, Inc., New York, NY, USA, 91–120.
- 408 Angulo, E., Castillo, E., Garcia-Rodenas, R., and Sanchez-Vizcaino, J. (2012). "Determining highway
409 corridors." *J. Transp. Eng.*, 10.1061/(ASCE)TE.1943-5436.0000361.
- 410 APA (Portuguese Environmental Agency). (2012). "Environmental Atlas.",
411 <<http://sniamb.apambiente.pt/webatlas/>>.
- 412 Bertsimas, D., and Nohadani, O. (2010). "Robust optimization with simulated annealing." *J. Global Optim.*,
413 48(2), 323–334.
- 414 Brons, M., Givoni, M., and Rietveld, P. (2009). "Access to railway stations and its potential in increasing rail
415 use." *Transport. Res. A-Pol.*, 43(2), 136–149.
- 416 Campos, J., and de Rus, G. (2009). "Some stylized facts about high-speed rail: A review of HSR experiences
417 around the world." *Transport Policy*, 16(1), 19–28.
- 418 CEN (European Committee for Standardization). (2002). "Railway application - Track alignment design
419 parameters - Track gauges 1435 mm and wider - Part 1: Plain Line." *ENV 13803-1*, Brussels.
- 420 Costa, A. L., Cunha, C., Coelho, P. a L. F., and Einstein, H. H. (2013). "Solving High-Speed Rail Planning with
421 the Simulated Annealing Algorithm." *J. Transp. Eng.*, 10.1061/(ASCE)TE.1943-5436.0000542, 635-642.
- 422 Cunha, M. C. (1999). "On solving aquifer management problems with simulated annealing algorithms." *Water*
423 *Resour. Manage.*, 13(3), 153–169.
- 424 Cunha, M. C., Pinheiro, L., Zeferino, J., Antunes, A., and Afonso, P. (2009). "Optimization Model for
425 Integrated Regional Wastewater Systems Planning." *J. Water Resour. Plann. Manage.*,
426 10.1061/(ASCE)0733-9496(2009)135:1(23).
- 427 EC (European Commission). (2008). "Commission Decision of 20 December 2007 concerning a technical
428 specification for interoperability relating to the infrastructure sub-system of the trans-European high-speed
429 rail system." *Off. J. Eur. Union*, <<http://eur-lex.europa.eu/>> (Nov. 30, 2011).

- 430 Jha, M. K., Schonfeld, P., and Samanta, S. (2007). "Optimizing rail transit routes with genetic algorithms and
431 geographic information system." *J. Urban Plann. Dev.*, 133(3), 161–171., 10.1061/(ASCE)0733-
432 9488(2007)133:3(161)
- 433 Jilla, C. D., and Miller, D. W. (2001). "Assessing the performance of a heuristic simulated annealing algorithm
434 for the design of distributed satellite systems." *Acta Astron.*, 48(5-12), 529–543.
- 435 Johnson, D. S., Aragon, C. R., McGeoch, L. A., and Schevon, C. (1989). "Optimization by Simulated
436 Annealing - An Experimental Evaluation . Part 1. Graph Partitioning." *Oper. Res.*, 37(6), 865–892.
- 437 Johnson, D. S., and McGeoch, L. A. (1997). "The traveling salesman problem: a case-study." *Local Search in
438 Combinatorial Optimization*, John Wiley & Sons Ltd, New York, NY, USA, 215–310.
- 439 Kang, M. W., Jha, M. K., and Schonfeld, P. (2012). "Applicability of highway alignment optimization models." *Transport. Res. C-Emer.*, 21(1), 257–286.
440
- 441 Kang, M. W., Jha, M. K., and Buddharaju, R. (2014). "Rail Transit Route Optimization Model for Rail
442 Infrastructure Planning and Design: Case Study of Saint Andrews, Scotland." *J. Transp. Eng.*, 140(1), 1–11. doi:
443 10.1061/(ASCE)TE.1943-5436.0000445
- 444 Kirkpatrick, S., Gelatt, C. D., and Vecchi, M. P. (1983). "Optimization by simulated annealing." *Science*,
445 220(4598), 671–680.
- 446 Van Laarhoven, P. J. M., and Aarts, E. H. L. (1987). *Simulated annealing: theory and applications*. Kluwer
447 Academic Publishers Group, Dordrecht, The Netherlands.
- 448 Levinson, D. M. (2012). "Accessibility impacts of high-speed rail." *Journal of Transport Geography*, 22(0),
449 288–291.
- 450 Maier, H. R., Kapelan, Z., Kasprzyk, J., Kollat, J., Matott, L. S., Cunha, M. C., Dandy, G. C., Gibbs, M. S.,
451 Keedwell, E., Marchi, A., Ostfeld, A., Savic, D., Solomatine, D. P., Vrugt, J. A., Zecchin, A. C., Minsker,
452 B. S., Barbour, E. J., Kuczera, G., Pasha, F., Castelletti, A., Giuliani, M., and Reed, P. M. (2014).
453 "Evolutionary algorithms and other metaheuristics in water resources: Current status, research challenges
454 and future directions." *Environ. Modell. Softw.*, 62, 271–299.
- 455 Marques, J., Cunha, M., and Savić, D. (2015). "Using Real Options in the Optimal Design of Water Distribution
456 Networks." *J. Water Resour. Plann. Manage.*, 10.1061/(ASCE)WR.1943-5452.0000448.
- 457 Metropolis, N., Rosenbluth, A. W., Rosenbluth, M. N., Teller, A. H., and Teller, E. (1953). "Equation of State
458 Calculations by Fast Computing Machines." *J. Chem. Phys.*, 21(6), 1087–1092.
- 459 Pardalos, P. M., Romeijn, H. E., and Tuy, H. (2000). "Recent developments and trends in global optimization." *J. Comput. Appl. Math.*, 124(1-2), 209–228.
460
- 461 Profillidis, V.A. (2006). *Railway management and engineering*, Ashgate Publishing Co.
- 462 RAVE. (2008). "High-Speed Rail Connection between Lisbon and Oporto." *Preliminary Project Design*,
463 Lisbon, Portugal.
- 464 Repolho, H. M., Antunes, A. P., and Church, R. L. (2013). "Optimal Location of Railway Stations: The Lisbon-
465 Porto High-Speed Rail Line." *Transp. Sci.*, 47(3), 330–343.
- 466 RTRI (Railway Research Technical Institute). (2007). *Design Standards for Railway Structures - Displacement
467 Limits*, Japan.
- 468 Samanta, S., and Jha, M. K. (2011). "Modeling a rail transit alignment considering different objectives." *Transport. Res. A-Pol.*, 45(1), 31–45.
469
- 470 SNIRH (Portuguese National Information System on Hydrological Resources). (2012). "Water Atlas",
471 <<http://geo.snirh.pt/AtlasAgua/>>.
- 472 Zeferino, J. A., Cunha, M. C., and Antunes, A. P. (2012). "Robust optimization approach to regional wastewater
473 system planning." *J. Environ. Manag.*, 109, 113–122.
- 474

475 **Figure Captions List**

476 **Fig. 1.** Case-study area (rectangle of $147.4 * 304.4\text{km}^2$) and cities represented by the (x;y;z) coordinates in
477 (km;km;m).

478 **Fig. 2.** Generation of HSR configurations: a) 3D neighborhood of a current (center) node and b) Plan view of
479 the perturbation of a current configuration (solid line) into a neighboring candidate configuration (dashed line).

480 **Fig. 3.** HSR configurations overlaying the protected land-use layer map: a) initial configuration and b) best
481 configuration found by the SAA implementation according to Costa et al. (2013).

482 **Fig. 4.** Transposing protected land-use areas a) successfully and b) unsuccessfully; and c) with the repositioning
483 of nodes N, (N-1) and (N+1).

484 **Fig. 5.** Transposing protected land-use areas: a) step 2 and b) step 3.

485 **Fig. 6.** Lisbon-Oporto rivers' map with the location of the cross-section line defining the upstream limits of the
486 70 meters bridge height requirement.

487 **Fig. 7.** Plan view showing evidence of HSR clustering, overlaying the Lisbon-Oporto land-use layer.

488 **Fig. 8.** Minimum length of linear sections linking nodes i, j and k of the HSR alignment with an horizontal angle
489 $\beta_{(i,j,k)}$, for a circular curve of 4500m radius and an external secant Δ .

490 **Fig. 9.** Plan view of HSR solution overlaid on the case-study maps: a) land-use, b) rivers, c) elevation.

491 **Fig. 10.** HSR longitudinal profile with indication of built extension on bridges and tunnels. Vertical
492 exaggeration of 150x.

493 **Fig. 11.** HSR plan view overlaying the expropriation cost map between Aveiro and Leiria with detail of the unit
494 expropriation costs ($\text{€}/\text{m}^2$) next to the Coimbra HSR station.

495 **Fig. 12.** Accumulated costs (in euros of 2008) along the HSR longitudinal profile: total construction costs and
496 partials for earthworks, expropriation, bridges, tunnels and length-dependent costs.

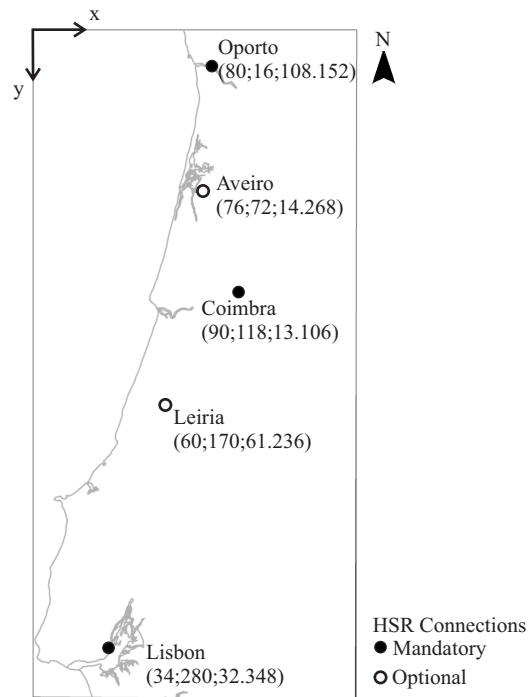


Fig. 1. Case-study area (rectangle of 147.4 * 304.4km²) and cities represented by the (x;y;z) coordinates in (km;km;m)

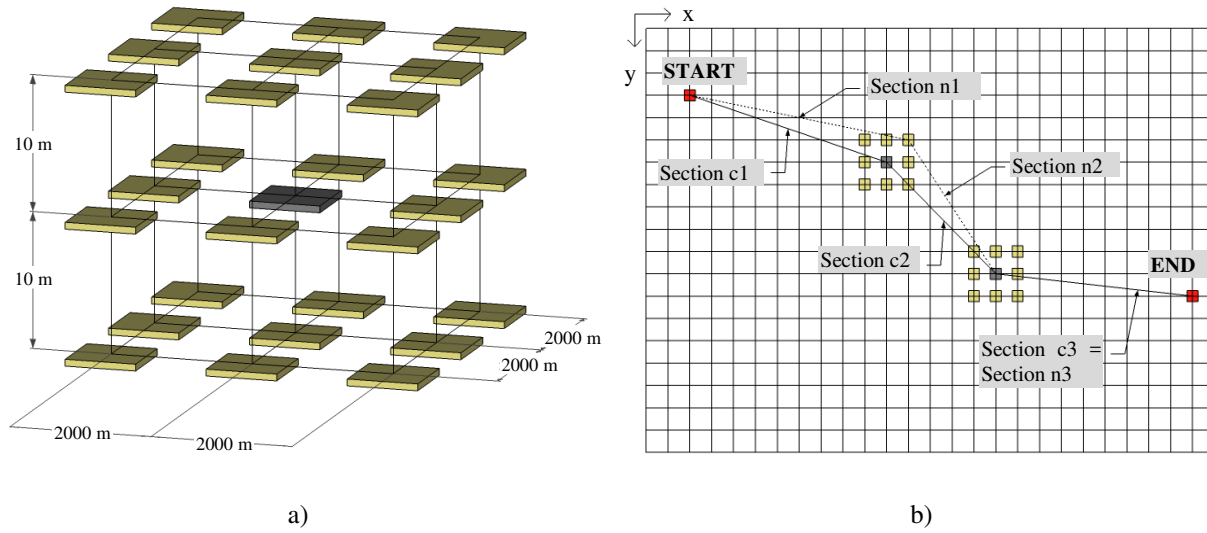


Fig. 2. Generation of HSR configurations: a) 3D neighborhood of a current (center) node and b) Plan view of the perturbation of a current configuration (solid line) into a neighboring candidate configuration (dashed line).

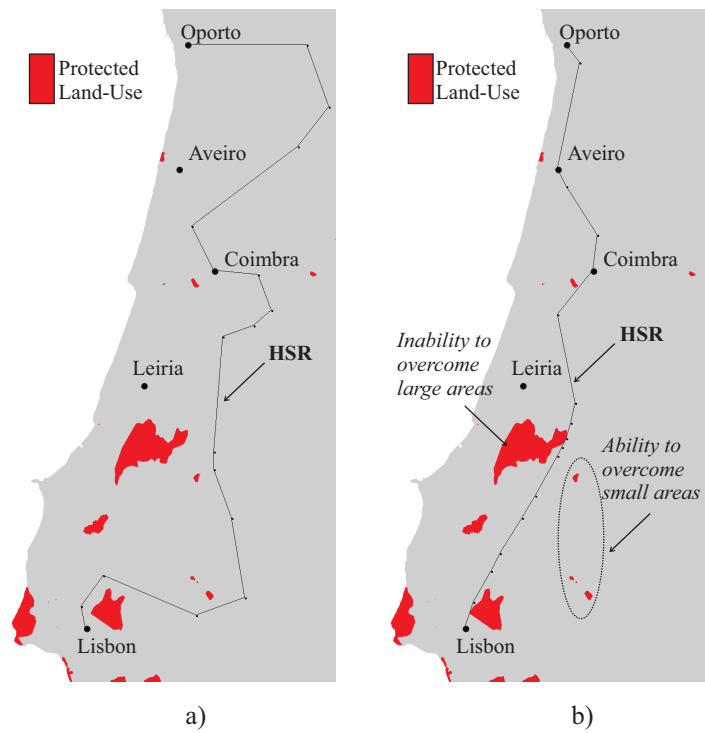


Fig. 3. HSR configurations overlaying the protected land-use layer map: a) initial configuration and b) best configuration found by the SAA implementation according to Costa et al. (2013).

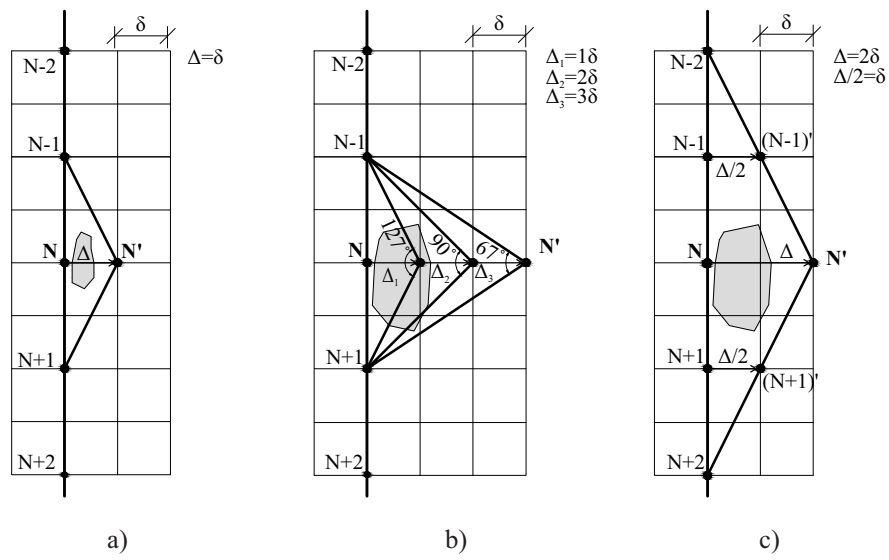


Fig. 4. Transposing protected land-use areas a) successfully and b) unsuccessfully; and c) with the repositioning of nodes N, (N-1) and (N+1).

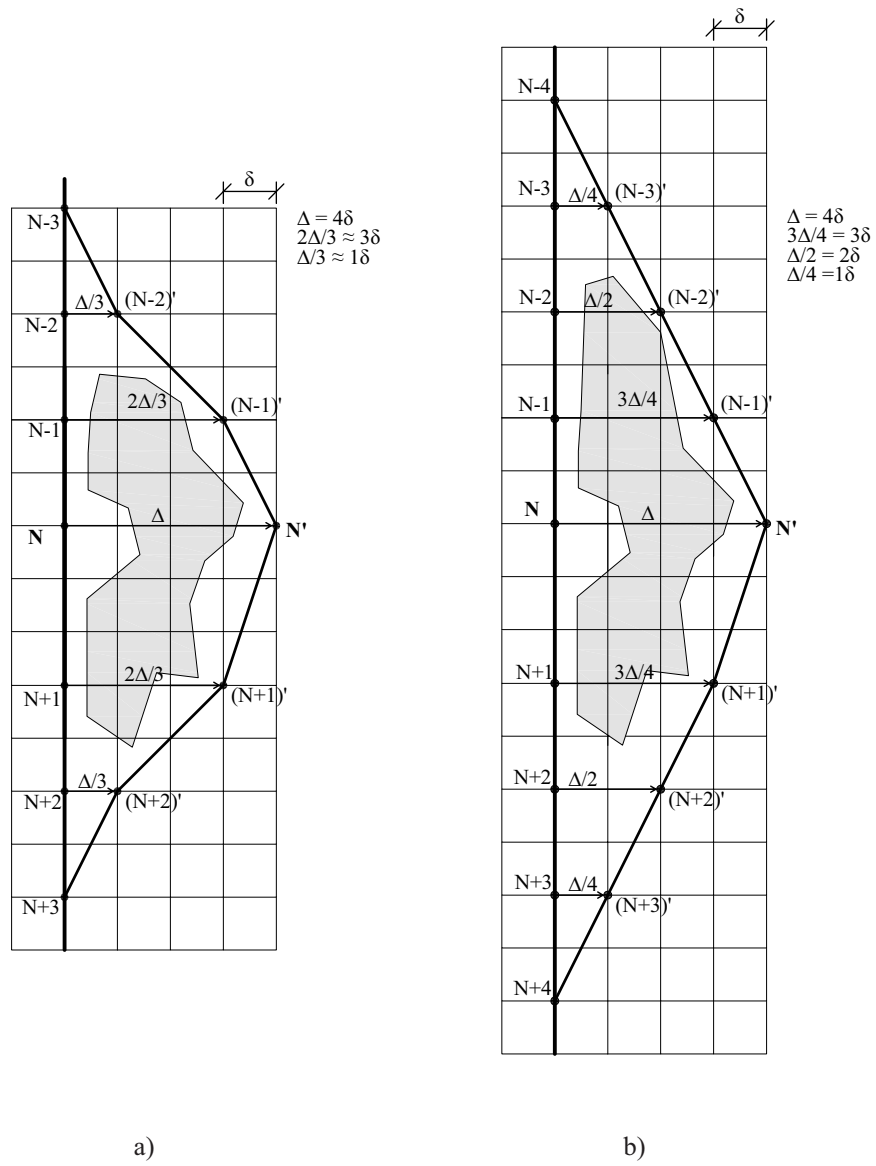


Fig. 5. Transposing protected land-use areas a) step 2 and b) step 3.



Fig. 6. Lisbon-Oporto rivers' map with the location of the cross-section line defining the upstream limits of the 70 meters bridge height requirement.

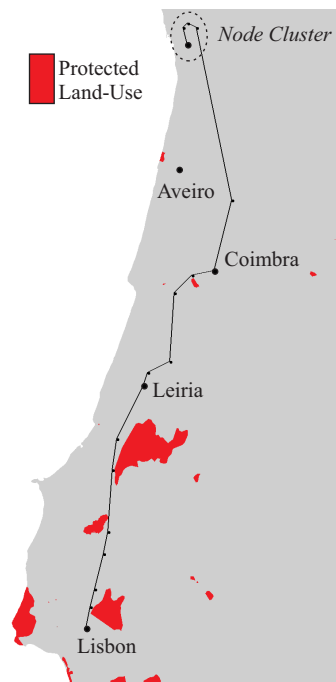


Fig. 7. Plan view showing evidence of HSR clustering, overlaying the Lisbon-Oporto land-use layer.

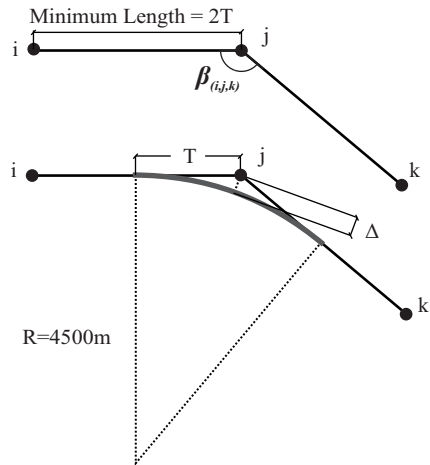


Fig. 8. Minimum length of linear sections linking nodes i , j and k of the HSR alignment with an horizontal angle $\beta_{(i,j,k)}$, for a circular curve of 4500m radius and an external secant Δ .

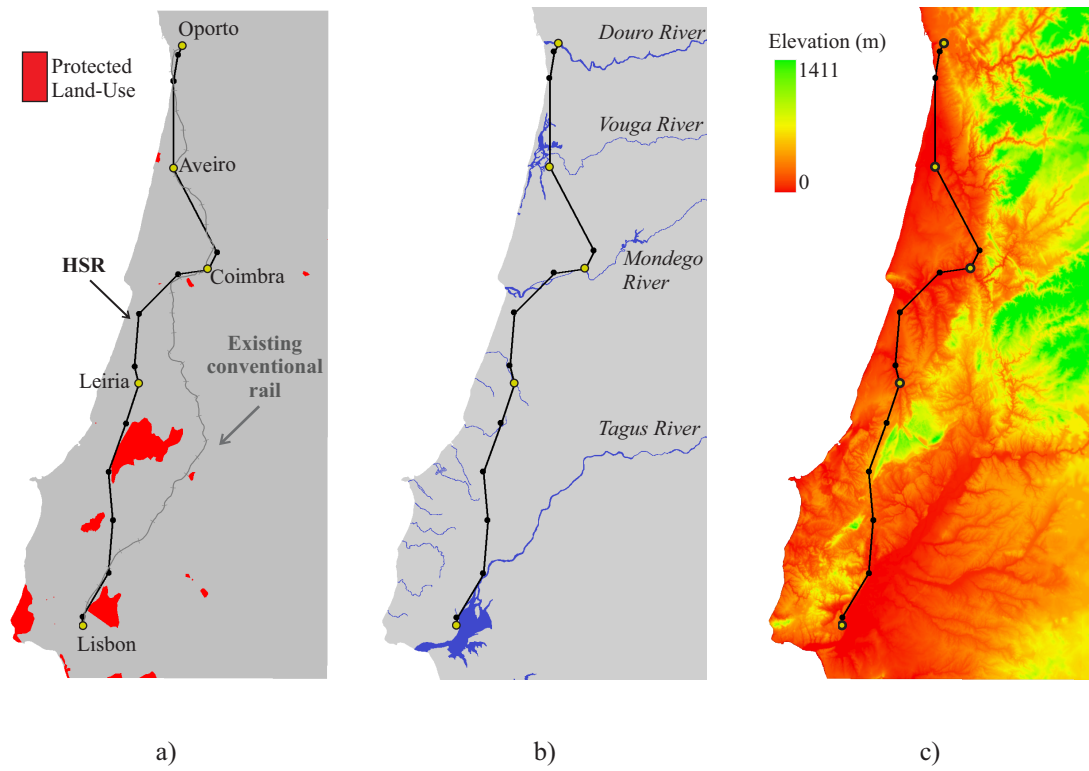


Fig. 9. Plan view of HSR solution overlaid on the case-study maps: a) land-use, b) rivers, c) elevation.

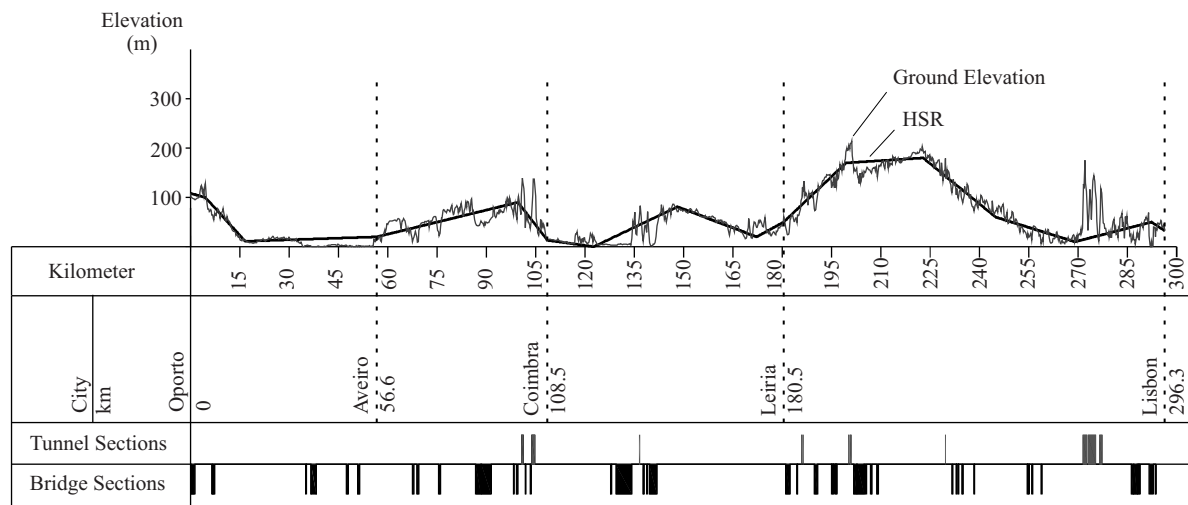


Fig. 10. HSR longitudinal profile with indication of built extension on bridges and tunnels. Vertical exaggeration of 150x.

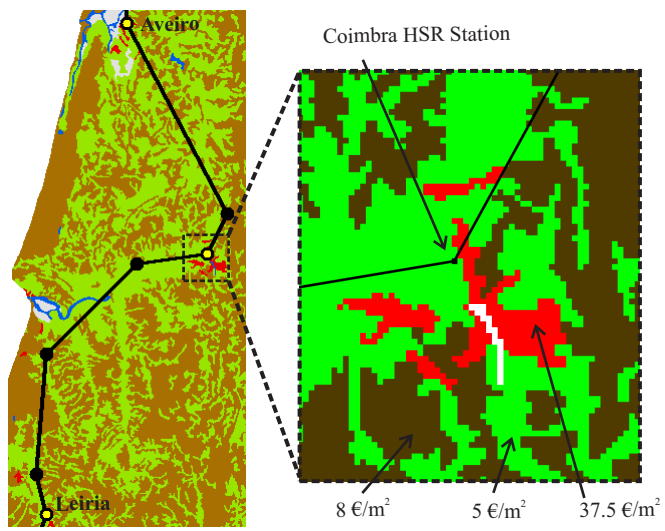


Fig. 11. HSR plan view overlaying the expropriation cost map between Aveiro and Leiria with detail of the unit expropriation costs (€/m²) next to the Coimbra HSR station.

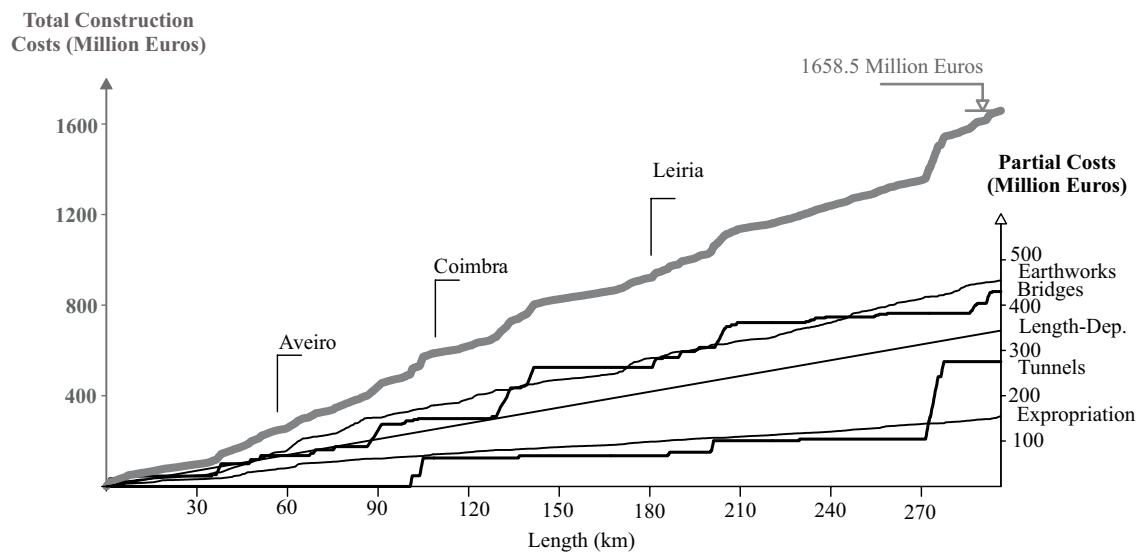


Fig. 12. Accumulated costs (in euros of 2008) along the HSR longitudinal profile: total construction costs and partials for earthworks, expropriation, bridges, tunnels and length-dependent costs.